



ELSEVIER

Earth and Planetary Science Letters 189 (2001) 103–114

EPSL

www.elsevier.com/locate/epsl

Reappraisal of the Arabia–India–Somalia triple junction kinematics

Marc Fournier^{a,*}, Philippe Patriat^b, Sylvie Leroy^a

^a CNRS ESA 7072, Laboratoire de Tectonique, Université Pierre et Marie Curie, Case 129, 4 place Jussieu, 75252 Paris cedex 05, France

^b Laboratoire de Géophysique Marine, Institut de Physique du Globe, 4 place Jussieu, 75252 Paris cedex 05, France

Received 12 March 2001; accepted 7 May 2001

Abstract

We propose alternative kinematics for the Arabia–India–Somalia triple junction based on a re-interpretation of seismological and magnetic data. The new triple junction of the ridge–ridge–ridge type is located at the bend of the Sheba Ridge in the eastern gulf of Aden at 14.5°N and 56.4°E. The Owen fracture zone (Arabia–India boundary) is connected to the Sheba Ridge by an ultra-slow divergent boundary trending N80°E ± 10° marked by diffuse seismicity. The location of the Arabia–India rotation pole is constrained at 14.1°N and 71.2°E by fitting the active part of the Owen fracture zone with a small circle. The finite kinematics of the triple junction is inferred from the present-day kinematics. Since the inception of the accretion 15–18 Ma ago, the Sheba Ridge has probably receded ~ 300 km at the expense of the Carlsberg Ridge which propagated northwestward in the gulf of Aden, while an ultra-slow divergent plate boundary developed between the Arabian and Indian plates. The overall geometry of the new triple junction is very similar to that of the Azores triple junction. © 2001 Elsevier Science B.V. All rights reserved.

Keywords: Indian Ocean; kinematics; triple junctions; Owen fracture zone

1. Introduction

Since the establishment in the early 1960s of the worldwide standardized seismographic network (WWSSN), the seismicity maps sharply define the plate boundaries and the triple junctions in the oceanic domain. The plate–motion models calculated since then account satisfactorily for the kinematics of these boundaries [1–3], and the

kinematics of the main triple junctions has been constrained with empirical data collected during geophysical surveys (e.g. [4–10]). However, the kinematics of the very slow plate boundaries and associated triple junctions with a low seismic activity remain poorly known. One of the slowest plate boundaries on Earth is the boundary between the Arabian and Indian plates in the Arabian Sea, made up of the Owen fracture zone and the Dalrymple Trough [11] (Fig. 1). Earthquake focal mechanisms along this boundary evidence a right-lateral strike-slip motion (Fig. 1) estimated at 2 mm yr⁻¹ by the plate–motion model NUVEL-1A [2,3]. All global models [1–3,12] and re-

* Corresponding author. Fax: +33-1-44-27-50-85;
E-mail: marc.fournier@lgs.jussieu.fr

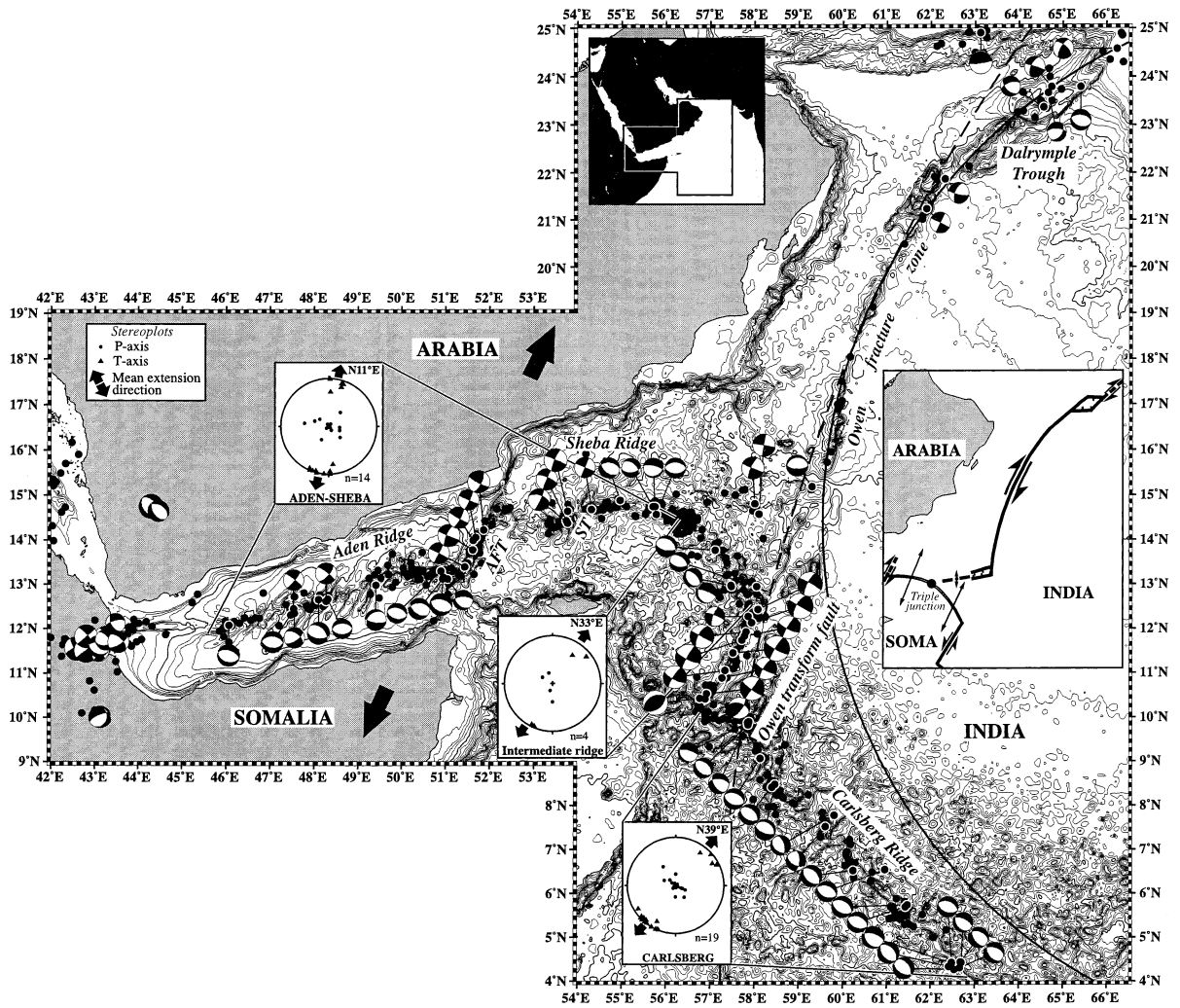


Fig. 1. Bathymetric map, shallow seismicity since 1973 (focal depth < 50 km; magnitude > 2; USGS/NEIC database), and all available earthquake focal mechanisms for the Arabia–India–Somalia triple junction region [11,16,17]. Inserted stereoplots give the equal-area projections of the P and T axes of the extensional focal mechanisms for the Carlsberg Ridge, the Aden-Sheba Ridge, and the intermediate ridge segment between the Carlsberg and Sheba ridges. The mean direction of extension (N33°E) along this ridge segment is similar to the direction of extension along the Carlsberg Ridge. Right insert shows the new geometry of the Arabia–India–Somalia triple junction. A small circle centered on the new Arabia–India pole (solid curve) fits better the Owen fracture zone than does a small circle centered on the NUVEL-1A Arabia–India pole (dashed curve). AFT is Alula-Fartak transform fault. ST is Socotra transform fault.

gional studies [11,13–15] assume that the Owen fracture zone extends southward up to the junction between the Sheba Ridge and the Owen transform fault where the Arabia–India–Somalia triple junction is classically located. However, the seismicity map shows that the southern Owen fracture zone is seismically quiet over approxi-

mately 250 km southward from 15°N and then does not seem to be an active plate boundary (Fig. 1). Furthermore, the entire Owen fracture zone cannot be satisfactorily fitted by a small circle centered on the Arabia–India pole of NUVEL-1A and going through the Arabia–India–Somalia triple junction [11] (Fig. 1). NUVEL-1A

Table 1
Source parameters of earthquake focal mechanisms

Date	Origin times (UT)	Latitude (°N)	Longitude (°E)	Depth (km)	Moment (dyne cm)	Plane 1			Plane 2			Source or reference	
						Strike (°)	Dip (°)	Rake (°)	Strike (°)	Dip (°)	Rake (°)		
<i>Owen fracture zone and Dairymple trough</i>													
March 30, 1966	4:18:39	21.870	62.320	20		200	60	-165	103	78	-30		[16]
April 4, 1968	1:44:24	24.580	66.230	12		210	70	150	310	64	145		[16]
Nov. 9, 1968	13:43:37	23.790	64.730	14		205	60	175	297	86	138		[16]
May 29, 1977	2:22:03	23.370	64.550	10	6.4e23	135	50	-39	252	61	-133		Harvard CMT
May 24, 1978	1:56:10	23.790	65.400	10	1.1e24	110	40	-80	277	50	-98		Harvard CMT
April 7, 1985	21:27:36	21.240	61.900	10	1.2e24	206	90	180	296	90	0		Harvard CMT
March 19, 1987	14:32:19	23.670	64.660	16	3.7e23	35	45	-138	272	62	-54		Harvard CMT
<i>New Arabia-India divergent plate boundary</i>													
Dec. 5, 1981	18:46:50	14.570	58.090	15	6.0e24	190	90	180	280	90	0		Harvard CMT
Dec. 14, 1985	18:13:31	14.800	58.000	10	4.9e24	204	76	-177	113	87	-14		Harvard CMT
Sept. 12, 1990	15:28:35	15.180	59.290	15	1.8e24	260	25	-101	92	65	-85		Harvard CMT
<i>Carlsberg Ridge</i>													
March 10, 1979	6:45:09	7.530	59.610	15	5.1e23	119	52	-142	3	61	-44		Harvard CMT
Jan. 3, 1980	18:11:51	0.040	67.180	15	1.2e25	306	41	-105	146	51	-77		Harvard CMT
Oct. 31, 1981	12:42:01	4.270	62.550	15	2.2e24	325	46	-70	118	47	-109		Harvard CMT
Jan. 5, 1985	6:43:35	-0.820	67.290	10	4.7e23	163	48	-56	298	52	-122		Harvard CMT
Jan. 5, 1985	7:39:09	-0.650	67.310	10	2.4e24	315	37	-108	157	55	-77		Harvard CMT
Oct. 18, 1985	16:55:30	4.430	62.710	10	5.4e23	143	31	-68	297	62	-103		Harvard CMT
Feb. 15, 1986	19:56:35	4.440	62.690	15	11.1e23	292	43	-116	146	52	-68		Harvard CMT
Aug. 8, 1986	16:18:56	7.780	59.810	15	5.7e24	128	36	-120	344	60	-70		Harvard CMT
Aug. 10, 1990	21:11:48	6.530	60.240	15	1.9e24	314	45	-90	134	45	-90		Harvard CMT
Sept. 28, 1992	23:49:28	4.430	62.490	15	8.3e23	291	45	-90	111	45	-90		Harvard CMT
March 20, 1993	6:30:26	9.830	57.850	15	6.4e23	310	45	-90	130	45	-90		Harvard CMT
March 19, 1994	10:43:34	8.480	58.460	15	10.4e23	309	29	-74	111	63	-99		Harvard CMT
May 25, 1994	22:10:35	6.550	60.970	15	1.0e24	293	45	-90	113	45	-90		Harvard CMT
May 25, 1994	22:13:32	5.700	61.430	15	1.2e24	293	45	-90	113	45	-90		Harvard CMT
May 26, 1994	0:30:07	5.750	61.480	15	1.9e24	300	45	-90	120	45	-90		Harvard CMT
July 8, 1994	17:10:13	0.200	66.710	15	1.2e24	302	79	177	33	87	11		Harvard CMT
July 8, 1995	11:39:05	4.330	62.420	15	3.0e24	317	45	-90	137	45	-90		Harvard CMT
Aug. 17, 1995	23:39:21	9.070	58.130	15	1.3e24	292	45	-90	112	45	-90		Harvard CMT
May 17, 1997	0:26:14	8.420	58.400	15	8.6e23	118	45	-100	312	46	-80		Harvard CMT
<i>Owen transform fault</i>													
May 30, 1978	20:17:15	11.050	57.330	15	9.8e24	118	74	168	212	79	17		Harvard CMT
April 20, 1980	2:37:49	11.740	57.710	15	5.6e25	116	75	172	208	83	15		Harvard CMT
April 8, 1983	2:28:25	11.450	57.510	10	6.2e25	211	80	9	119	81	170		Harvard CMT
July 29, 1983	18:03:59	10.410	56.880	10	1.7e24	289	49	154	37	71	44		Harvard CMT
July 7, 1986	16:26:56	10.420	56.760	15	4.0e25	242	42	98	52	48	83		Harvard CMT

Table 1 (continued)

Date	Origin times (UT)	Latitude (°N)	Longitude (°E)	Depth (km)	Moment (dyne cm)	Plane 1			Plane 2			Source or reference
						Strike (°)	Dip (°)	Rake (°)	Strike (°)	Dip (°)	Rake (°)	
Sept. 17, 1986	21:25:15	10.520	56.910	15	2.3e25	126	81	-179	36	89	-9	Harvard CMT
Feb. 26, 1992	3:45:19	11.830	57.770	15	9.3e24	117	76	170	210	81	14	Harvard CMT
Dec. 6, 1992	1:43:53	10.880	57.260	15	3.8e24	212	75	14	119	76	164	Harvard CMT
May 26, 1995	3:11:10	12.130	57.930	15	6.1e25	210	64	0	120	90	154	Harvard CMT
June 5, 1995	23:15:43	12.270	57.850	15	7.6e23	199	75	-11	292	79	-164	Harvard CMT
March 28, 1996	7:28:28	11.920	57.810	15	1.6e25	208	64	2	118	89	154	Harvard CMT
Oct. 1, 1996	15:50:23	12.430	58.070	15	4.9e25	207	73	-7	299	83	-163	Harvard CMT
<i>Northwestern segment of the Carlsberg Ridge</i>												
Jan. 26, 1980	1:00:49	13.760	57.100	15	1.8e24	307	33	-69	102	59	-103	Harvard CMT
July 10, 1988	2:42:54	12.970	57.460	15	2.8e23	151	35	-76	314	57	-100	Harvard CMT
July 1, 1995	4:10:55	12.940	57.470	15	10.4e23	161	23	-43	291	75	-107	Harvard CMT
Dec. 1, 1997	0:43:41	12.940	58.040	15	4.8e23	312	47	-65	97	49	-114	Harvard CMT
<i>Aden and Sheba ridges</i>												
Feb. 28, 1977	8:43:55	14.880	54.950	10	10.0e23	274	48	-118	132	49	-63	Harvard CMT
Dec. 17, 1977	23:57:54	13.130	50.940	15	1.8e24	270	45	-117	226	51	-66	Harvard CMT
Feb. 11, 1978	12:54:21	13.160	50.950	15	4.0e24	116	39	-79	282	52	-99	Harvard CMT
July 8, 1979	4:09:10	14.640	53.770	15	8.7e24	203	80	178	293	88	10	Harvard CMT
Sept. 24, 1979	23:41:36	12.670	48.320	15	6.8e23	268	45	-90	88	45	-90	Harvard CMT
Dec. 22, 1979	15:43:34	13.780	51.620	15	6.3e24	204	73	-176	113	86	-17	Harvard CMT
Dec. 8, 1982	6:19:37	12.080	46.060	14	3.2e24	105	39	-93	288	51	-88	Harvard CMT
Jan. 28, 1984	22:47:51	14.220	51.870	10	4.8e24	25	69	170	118	81	21	Harvard CMT
May 23, 1986	9:51:24	12.660	48.110	15	4.5e24	314	44	-62	98	52	-114	Harvard CMT
June 16, 1987	22:04:06	14.740	55.690	15	4.1e23	310	49	-56	84	51	-123	Harvard CMT
July 16, 1988	8:42:02	13.990	51.630	15	3.1e24	28	76	175	119	85	14	Harvard CMT
Nov. 24, 1989	7:22:26	12.620	48.280	15	1.9e24	41	67	-168	307	79	-24	Harvard CMT
Sept. 14, 1990	20:40:18	13.400	51.440	15	2.0e24	207	90	-180	297	90	0	Harvard CMT
Nov. 3, 1990	11:20:19	14.670	54.300	15	8.7e23	212	90	-180	302	90	0	Harvard CMT
May 11, 1991	15:26:29	12.450	47.540	15	1.4e24	308	82	-8	40	82	-172	Harvard CMT
May 12, 1991	16:12:37	12.310	47.470	15	2.0e24	275	45	-90	95	45	-90	Harvard CMT
May 21, 1992	4:13:17	13.300	50.900	15	7.7e23	284	45	-90	104	45	-90	Harvard CMT
Jan. 8, 1993	17:31:10	12.990	49.410	15	1.9e24	231	30	-134	99	69	-68	Harvard CMT
Oct. 12, 1993	21:04:52	13.130	51.050	15	6.8e23	137	37	-48	269	63	-117	Harvard CMT
Nov. 9, 1993	2:14:04	14.430	53.740	15	2.9e24	294	75	3	203	87	165	Harvard CMT
Dec. 7, 1995	17:48:16	14.560	55.770	15	.9e24	272	45	-90	92	45	-90	Harvard CMT
March 14, 1996	21:47:57	14.740	55.740	15	7.0e23	72	20	-118	282	72	-80	Harvard CMT
June 7, 1997	11:22:03	14.060	51.690	15	1.4e24	24	81	177	114	87	9	Harvard CMT
Jan. 1, 1998	19:17:16	14.370	53.770	15	3.5e24	290	58	-9	25	82	-148	Harvard CMT
Nov. 23, 1998	19:16:45	12.350	47.560	15	1.4e24	305	53	-33	56	64	-138	Harvard CMT

thus predicts a right-lateral motion with a normal slip component at the southern end of the Owen fracture zone which is not documented by seismological data. In the following, we re-examine regional seismological and magnetic data and propose a new location and new kinematics for the Arabia–India–Somalia triple junction.

2. The Arabia–India plate boundary

46 earthquakes of magnitude greater than 2 have occurred since 1973 along the Owen fracture zone and the Dalrymple Trough (US National Earthquake Information Center) and height focal mechanisms [16] and Harvard CMT solutions [17] have been computed for earthquakes with magnitudes greater than 5.5 (Fig. 1 and Table 1). The most active part of the plate boundary is the Dalrymple Trough. This trough consists of two basins, a long and narrow basin along the Owen fracture zone to the south and a rhomboedric shaped basin to the north. The rhomboedric basin is bounded to the east and the west by scarps parallel to the N45°E trending Owen fracture zone and to the south and the north by E–W trending scarps. Extensional and strike-slip earthquakes occurred in the northern basin [11]. The dominantly strike-slip focal mechanisms are consistent with right-lateral strike slip parallel to the Owen fracture zone. The extensional mechanisms are consistent with normal slip along E–W trending fault planes. One strike-slip event between the Dalrymple Trough and the Pakistan coast is also consistent with right-lateral slip along the north-eastern extent of the Owen fracture zone. This overall deformation pattern suggests that the northern Dalrymple Trough is a right-lateral pull-apart basin (right insert in Fig. 1).

South of the Dalrymple Trough, two strike-slip focal mechanisms between latitudes 21°N and 22°N indicate a consistent sense of right-lateral slip along the Owen fracture zone. The fracture zone is seismically active up to the 15°N latitude, but is totally devoid of seismicity farther south up to the Owen transform fault (Fig. 1). Indeed, the seismic zone turns towards the west at 15°N and joins the Sheba Ridge at 56°E. Its mean trend

between the Owen fracture zone and the Sheba Ridge is N80°E ± 10°. It starts to the east with an E–W trending trough about 1000 m deep, where a normal faulting earthquake consistent with N–S extension occurred (Fig. 1). Farther west, two strike-slip earthquakes are consistent with right-lateral strike slip parallel to the Owen fracture zone [11]. The seismic zone terminates to the west by a large seismic swarm at the junction with the Sheba Ridge.

This seismic zone is a segment of the Arabia–India plate boundary. The extensional focal mechanism close to the Owen fracture zone indicates that the Arabian plate is moving northward with respect to the Indian plate along this boundary segment. This motion is consistent with the right-lateral sense of slip along the Owen fracture zone. The plate boundary segment thus is of the divergent type. The trough at its eastern extremity can be regarded as a tension fracture at the end of the right-lateral Owen fracture zone. The two strike-slip focal mechanisms farther west may reveal the presence of a minor transform fault. We propose that the seismic swarm at the junction with the Sheba Ridge indicates the location of the Arabia–India–Somalia triple junction (at ~14.5°N and 56.4°E).

3. Kinematics and strain of the Aden–Sheba and Carlsberg ridges

If the above interpretation is correct, the ridge segment located between the former and the new Arabia–India–Somalia triple junction should rather belong to the Carlsberg Ridge than to the Sheba Ridge. The two ridges are very similar in terms of spreading rate and direction as predicted by NUVEL-1A: 22.7 mm yr⁻¹ along N23°E for the Sheba Ridge at 14.7°N and 55°E, and 23.1 mm yr⁻¹ along N30°E for the Carlsberg Ridge at 10°N and 57°E. The mean directions of the strike-slip earthquake slip vectors along the main transform faults are also very close: N25°E ± 5° for the slip vectors of the Alula–Fartak [18] and Socotra transform faults (Sheba Ridge) and N28°E ± 4° for those of the Owen transform fault (Carlsberg Ridge). The main dif-

ference between the two ridges is their general orientation. The Sheba Ridge trends $N90^{\circ}E \pm 5^{\circ}$ in the vicinity of the new triple junction, whereas the Carlsberg Ridge trends $N130^{\circ}E \pm 5^{\circ}$. Consequently, the principal strain directions along the two ridges, determined from the P, N, and T seismic axes of the extensional focal mechanisms, are also different since they depend on the spreading direction and the ridge strike [19–21]. The mean direction of extension is $N11^{\circ}E$ along the Aden–Sheba Ridge between longitudes $46^{\circ}E$ and $56^{\circ}E$ (14 mechanisms), and $N39^{\circ}E$ along the Carlsberg Ridge between longitudes $57^{\circ}E$ and $63^{\circ}E$ (19 mechanisms; stereoplots in Fig. 1; Table 1). The trend of the intermediate ridge segment between the former and the new triple junction is $\sim N130^{\circ}E$ and the extension direction along this segment is $N33^{\circ}E$ (four mechanisms; Fig. 1), which is similar to the extension direction along the Carlsberg Ridge. Thus, this segment seems to pertain to the Carlsberg Ridge, which is in line with the new geometry of the triple junction discussed above. In Table 1 and in the following, we shall refer to this ridge segment as the northwest segment of the Carlsberg Ridge.

The new geometry of the triple junction also implies that the southern part of the Owen fracture zone is not an active plate boundary. It could represent the fossil trace of the Owen transform fault.

4. Kinematics of the Arabian and Indian plates

We revised the Arabia–India kinematics taking into account the modification of the geometry of the plate boundary. The Owen fracture zone is assumed to be a pure strike-slip boundary from $15^{\circ}N$ to $23^{\circ}N$ and therefore must lie on a small circle centered on the Arabia–India pole. We fitted with the best small circle (in the least-square sense) the epicenters of the 46 earthquakes which occurred along the Owen fracture zone and the Dalrymple Trough since 1973, and the bathymetric crest of the Owen fracture zone between $15^{\circ}N$ and $23^{\circ}N$ (10 points). The center of the resulting best small circle is located at $14.1^{\circ}N$ and $71.2^{\circ}E$ and its radius is 11.5° (standard error 0.15°). This

small circle (solid curve in Fig. 1) fits better the Owen fracture zone than does the small circle centered on the Arabia–India pole of NUVEL-1A (dotted curve in Fig. 1), which fits well the Owen fracture zone between $17^{\circ}N$ and $21^{\circ}N$, but not so well farther to the north and to the south. The new pole is within the 1σ error ellipse of the NUVEL-1A Arabia–India pole (Fig. 2).

The location of the Arabia–India pole can be independently obtained from the intersection of the great circles perpendicular to the slip vectors of the strike-slip earthquakes along the plate boundary [22]. For the five predominantly strike-slip earthquakes of the Owen fracture zone, we took the fault plane to be the nodal plane closest in strike to the fracture zone. Most of the great circles intersect between $15^{\circ}N$ and $22^{\circ}N$ and between $67^{\circ}E$ and $76^{\circ}E$ (Fig. 2). This result is in reasonable agreement with the location of the Arabia–India pole determined above, which is closer to the intersection zone of the great circles than the NUVEL-1A pole.

The Arabia–India angular velocity can be deduced from the velocity triangle at the Arabia–India–Somalia triple junction. For this purpose, we used recent magnetic profiles along the Carlsberg [23,24] and Aden [25,26] ridges, which were unavailable for previous studies [2,11,14], to constrain the present-day India–Somalia and Arabia–Somalia Euler vectors.

5. India–Somalia and Arabia–Somalia kinematics

The clear shape of the anomaly A2 on the flanks of the Carlsberg and Aden–Sheba ridges

Table 2
Arabia–India–Somalia Euler vectors

Plate pair	Latitude $^{\circ}N$	Longitude $^{\circ}E$	ω $^{\circ} \text{myr}^{-1}$	Reference
in-so	23.60	29.70	0.430	this work
in-af	23.6	28.5	0.41	[3]
ar-so	24.01	24.57	0.393	this work
ar-af	24.1	24.0	0.40	[3]
in-ar	14.10	71.20	0.050	this work
in-ar	3.0	91.5	0.03	[3]

in = India, so = Somalia, af = Africa, ar = Arabia.

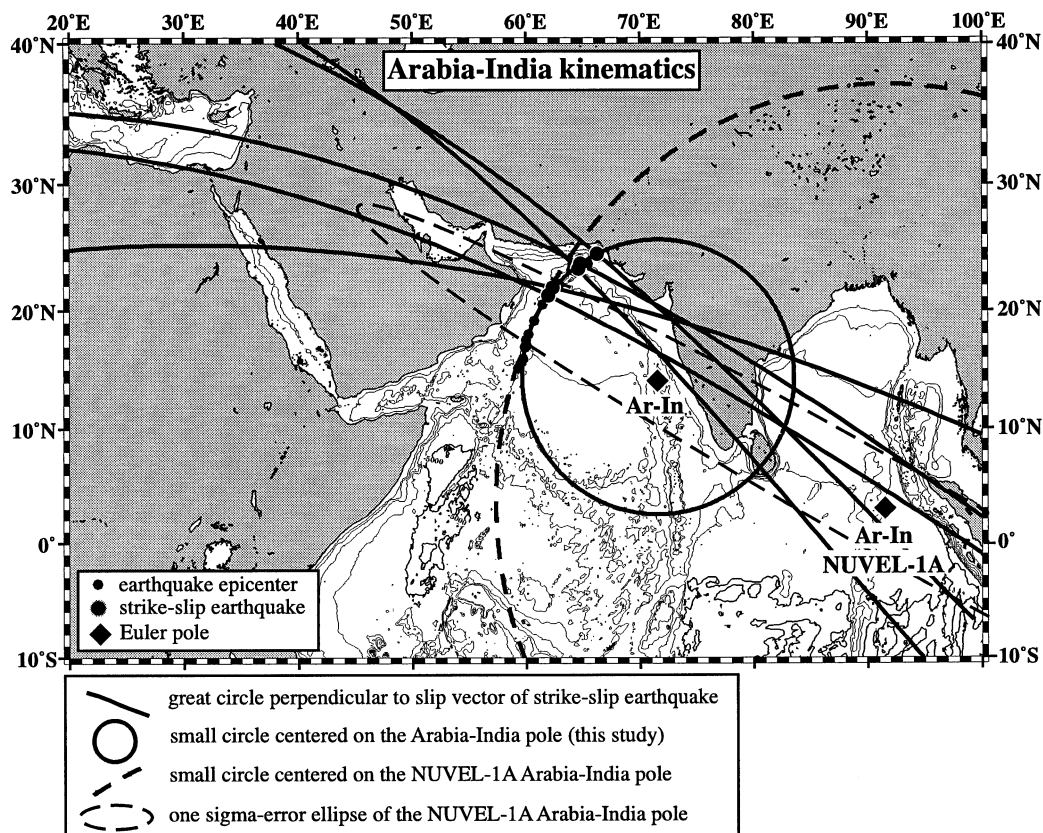


Fig. 2. The Arabia–India pole is located at the center of a small circle (solid circle) that best fits the seismicity and the bathymetric crest of the Owen fracture zone. It is within the 1σ error ellipse of the NUVEL-1A Arabia–India pole. The great circles (solid curves) perpendicular to the slip vectors of five predominantly strike-slip earthquakes along the Arabia–India plate boundary intersect in the vicinity of the new pole.

makes easy its unambiguous identification. However, for low spreading rates of the order of 10 mm yr^{-1} as in the western gulf of Aden, it is not always well developed. After discarding the ambiguous profiles, we carefully picked the anomalies A2 (old edge of the Olduvai subchron) along each original profile. The quality of the resultant isochron map (Fig. 3A and B) is relevant to the density of the picks, being satisfactory for the Carlsberg Ridge and poor for the Aden–Sheba Ridge. The picks along the Aden–Sheba Ridge are indeed unevenly distributed on either side of the ridge, and some of them come from old cruises navigated without satellite positioning system. Nevertheless, the few good data used for the superposition are fortunately located at the two ends of the ridge, which guarantees a proper result.

First, the rotation vectors were determined by fitting the isochrons without the use of transform faults and earthquake focal mechanisms. A fit criterion (minimization of the triple vectorial product [27]) was computed for each solution and the fit criteria were contoured and plotted in Fig. 3C and D. The acceptable rotation vectors correspond to the best fit values. Second, the location of the poles was constrained with the great circles perpendicular to the slip vectors of the strike-slip earthquakes along the Alula–Fartak and Socotra transform faults for the Sheba Ridge and along the Owen transform fault for the Carlsberg Ridge (Fig. 3C and D). This kinematic constrain combined with the previous magnetic constrain allowed to drastically restrict the possible location of each pole. Third, the sum of the Arabia–Soma-

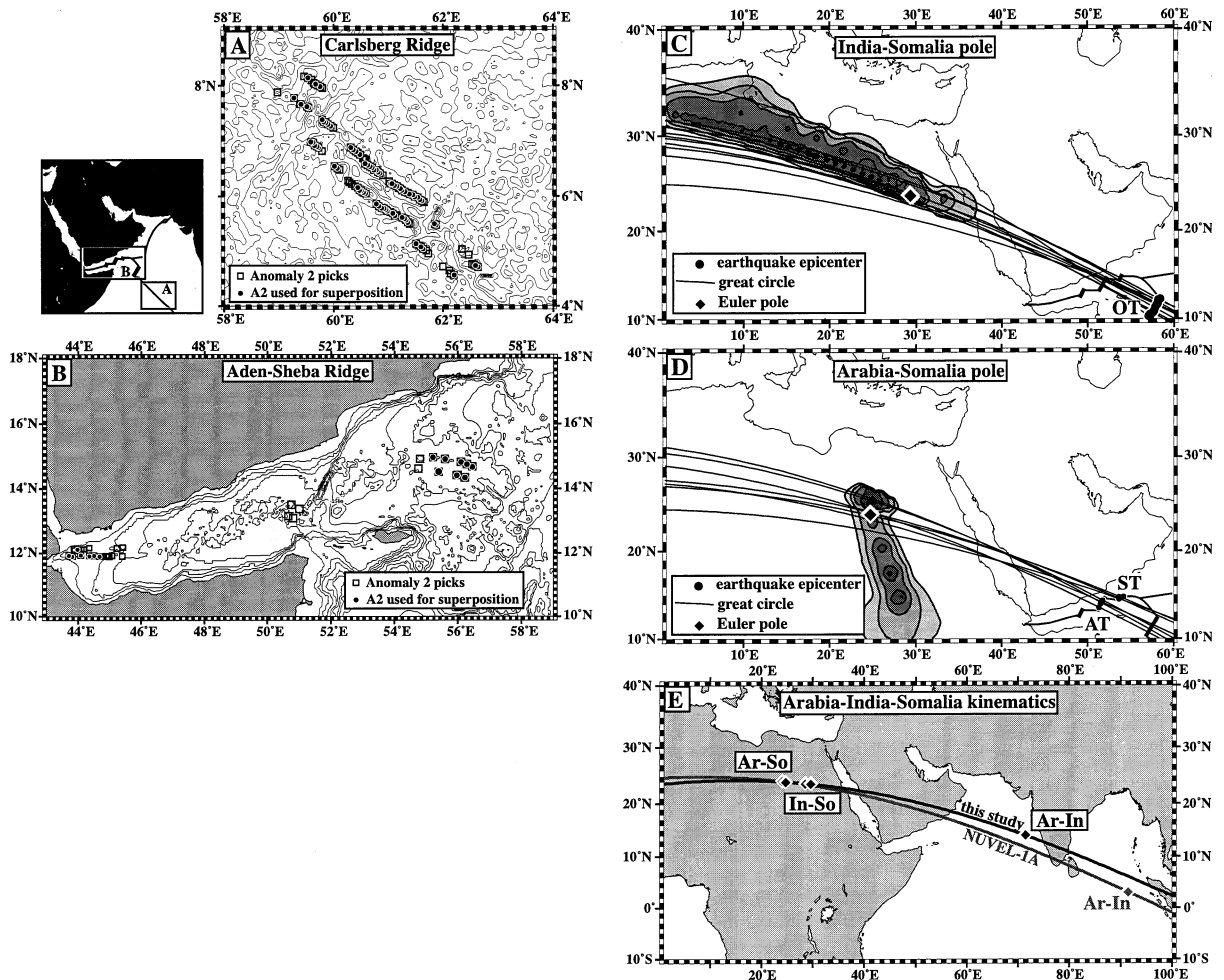


Fig. 3. Determination of the India–Somalia and Arabia–Somalia Euler vectors. (A and B) Geographic plot of the magnetic anomaly A2 picks on the flanks of the Carlsberg and Aden–Sheba ridges. (C and D) Contoured fit criteria computed by fitting the isochrons of anomaly A2, and great circles perpendicular to the slip vectors of the strike-slip earthquakes along the Owen (OT), Alula–Fartak (AT), and Socotra (ST) transform faults. The Euler poles are located in the intersection zones of the great circles and the best fit values (in black). (E) Best solution for the Arabia–India–Somalia kinematics compared with the NUVEL-1A solution (Table 2).

lia and Somalia–India rotation vectors must be collinear to the newly determined Arabia–India pole. The best solution is given in Table 2 and compared with the NUVEL-1A solution in Fig. 3E. The main difference between the two models is the location of the Arabia–India pole, the misfit between the magnitudes of the Arabia–Somalia (Arabia–Africa in NUVEL-1A) and India–Somalia (India–Africa) rotation vectors being lower than 5%. The Arabia–India rate of motion pre-

dicted along the Owen fracture zone is 1.1 mm yr^{-1} , which is in agreement with the slip rate predicted by NUVEL-1A between 0.2 mm yr^{-1} and 7 mm yr^{-1} .

6. Kinematics of the Arabia–India–Somalia triple junction

The former Arabia–India–Somalia triple junc-

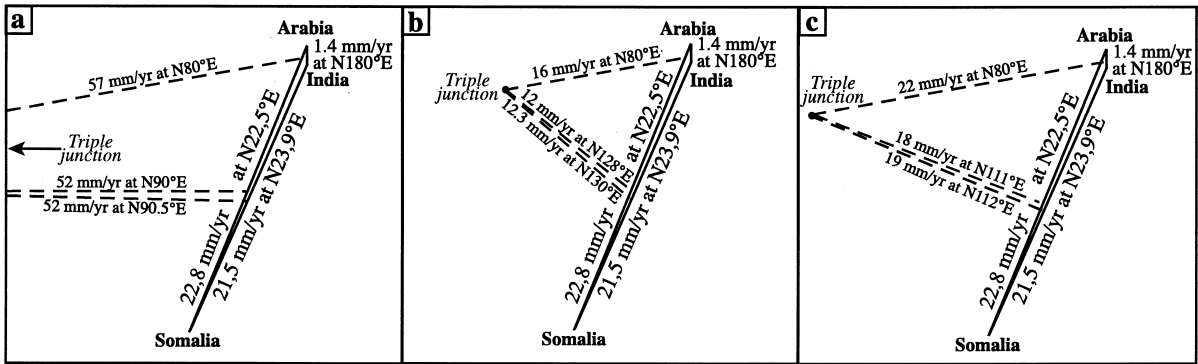


Fig. 4. Velocity triangle and stability of the new RRR triple junction. The dashed lines represent velocities which leave the geometry of the boundaries unchanged. Two extreme configurations are shown: (a) the Sheba and the northwestern Carlsberg ridges strike $\sim N90^\circ E$ at the triple junction and (b) the Sheba and the northwestern Carlsberg ridges strike $\sim N130^\circ E$ at the triple junction. The intermediate configuration (c) is calculated in the hypothesis that the triple junction has been stable since the inception of the accretion in the eastern gulf of Aden 15–18 Ma ago.

tion located at the northern end of the Owen transform fault involved two transform faults and one ridge (FFR triple junction). It was considered to be stable because the two transform faults have the same strike ($\sim N30^\circ E$). The triple junction proposed in this work is of the stable ridge–ridge–ridge type (RRR; Fig. 1). The velocity–space diagram calculated from the rotation vectors determined above is very flat because the spreading rates and directions along the Sheba and northwestern Carlsberg ridges are very close. The Arabia–India relative plate velocity is esti-

mated at 1.4 mm yr^{-1} along $N180^\circ E$ (Fig. 4). The triple junction traces on the adjacent plates do not appear on the marine gravity field map [28] and cannot be used to estimate the velocity of the triple junction relative to the African, Arabian, and Somalia plates. At the regional scale, the orientations of the three plate boundaries at the triple junction are $N90^\circ E \pm 5^\circ$ for the Sheba Ridge, $N130^\circ E \pm 5^\circ$ for the northwestern segment of the Carlsberg Ridge, and $N80^\circ E \pm 10^\circ$ for the Arabia–India plate boundary. It is possible to have these three ridge orientations meeting at a

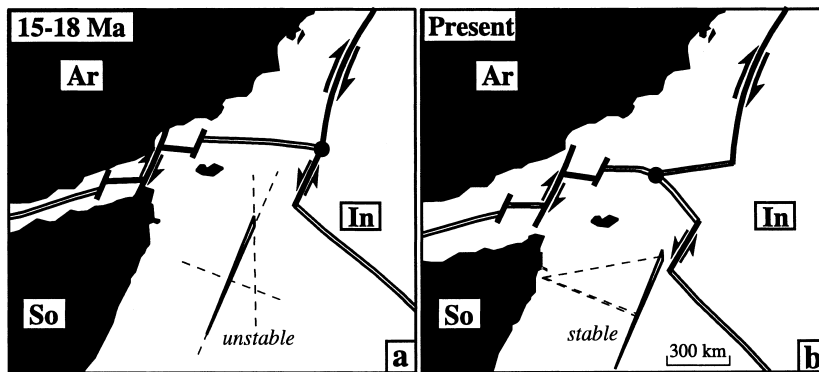


Fig. 5. Evolution of the Arabia–India–Somalia triple junction during the opening of the gulf of Aden. (a) Possible configuration at the beginning of the opening 15–18 Ma ago. The present-day Arabia–Somalia pole was used for the reconstruction (relative to stable Arabia). The nascent Sheba Ridge probably connected with the Owen fracture zone. The unstable FFR triple junction evolved in the stable RRR triple junction (b) which still prevails today. Since then, the Carlsberg Ridge propagated about 300 km northwestward at the expense of the Sheba Ridge, and the slow Arabia–India boundary lengthened 360 km.

point in the space–velocity diagram within the uncertainty bounds, but spreading on one or either of the Sheba or northwestern Carlsberg ridges must be very asymmetric. This asymmetry is not confirmed by the few magnetic profiles available around the triple junction, where the spreading appears nearly symmetrical. Assuming that the spreading has been symmetrical, the two ridges must be almost collinear at the triple junction. Two extreme geometries of the triple junction can then be considered with both ridges trending $\sim N90^\circ E$ in the first case (Fig. 4a) and $\sim N130^\circ E$ in the second case (Fig. 4b). For both configurations, the triple junction moves west with respect to the adjacent plates, and the Arabia–India plate boundary and the Carlsberg Ridge propagate westward at the expense of the Sheba Ridge. In the first case, the Sheba Ridge recedes at 52 mm yr^{-1} (Fig. 4a), a too large value when extrapolated to the whole duration of opening of the gulf of Aden (i.e. since 15–18 Ma [13,29,30]). In the second case, the Sheba Ridge recedes at 12 mm yr^{-1} (Fig. 4b).

An intermediate geometry of the triple junction can be obtained considering that it has been stable, in the sense of McKenzie and Morgan [31], since the inception of the accretion in the eastern gulf of Aden 15–18 Ma ago. The closing of the gulf of Aden requires a westward migration of the triple junction with respect to the three adjacent plates (Fig. 5). When the accretion started, it is likely that the Sheba Ridge connected with the Owen fracture zone (Fig. 5a). Since then, the triple junction migrated westward, the Arabia–India plate boundary lengthened $\sim 360 \text{ km}$, and the Carlsberg Ridge propagated about 300 km northwestward in the gulf of Aden at the expense of the Sheba Ridge (Fig. 5b). The propagation rate of the Arabia–India boundary would thus range from 20 to 24 mm yr^{-1} and that of the Carlsberg Ridge from 17 to 20 mm yr^{-1} . Assuming mean values of 22 mm yr^{-1} and 19 mm yr^{-1} for the propagation rates, the azimuths of the Carlsberg and Sheba ridges at the triple junction are constrained at $112^\circ E$ and $111^\circ E$, respectively, in the hypothesis of symmetrical and orthogonal spreading (Fig. 4c). In this configuration, the triple junction moves

west relative to the Arabian and Indian plates at $\sim 20 \text{ mm yr}^{-1}$.

7. Discussion and conclusion

Even if the triple junction has been stable since 15–18 Ma, the amount of finite extension along the ultra-slow Arabia–India plate boundary would not exceed 30 km at its eastern end near the Owen fracture zone, where it is the largest. It is suggested that because the relative motion between the Arabian and Indian plates was very slow, the diffuse extension never gave birth to a new spreading center. Alternatively, the ultra-slow boundary could be a young crack in the Arabian plate and the present geometry of the triple junction could be transient. In any case, a geophysical survey involving seismics and multibeam sonar is urgently needed to image the extension zone predicted by our model.

Mitchell (personal communication) noticed that numerous similarities exist between the Arabia–India–Somalia and the Azores triple junctions, in terms of both overall geometry of the plate boundaries and of their plate velocity–space diagrams. The Azores triple junction consists of a long transform fault, the Gloria fault, which ends westwards in an obliquely opening rift called the Teiceira Rift connecting the transform fault to the Mid-Atlantic Ridge (MAR) [4,32–34], just as the ultra-slow Arabia–India plate boundary connect the Owen fracture zone to the Sheba Ridge. The velocity–space diagrams of the two triple junctions are very similar, with two slow spreading ridges having similar rates and directions, and one ultra-slow spreading boundary forming the third arm [4]. The MAR changes its general orientation at the point where the Terceira Rift joins it, just as the Sheba Ridge changes its orientation at the junction with the ultra-slow rift. The Terceira Rift comprises a series of basins including the Formigas Trough which occurs at the end of the active Gloria transform fault, just as a basin occurs at the southern end of the Owen fracture zone. Therefore, the large-scale geometry of the Azores triple junction is strikingly similar to that of the Arabia–India–Somalia triple junction.

Moreover, the triple junction active when Iberia was moving independently from Eurasia at the time of opening of King's Trough (from ~ 44 to 25 Ma) also had a similar geometry to the Arabia–India–Somalia and Azores triple junctions, with an oblique rift (King's Trough) connecting a transform fault to the MAR [35]. This geometry thus seems to be common in a context of connection of a transform fault with a spreading ridge. It is likely that the RRR configuration with an ultra-slow rift is more stable than the RRF configuration.

Acknowledgements

We thank N.C. Mitchell for his thorough and constructive review that helped improve the original manuscript, and P. Huchon for his particular review. We also thank C. Norgeot for stimulating discussions at the initiation of this work and P. Agard for improving the English. Figures were drafted using GMT software [36]. *[ACJ]*

References

- [1] J.B. Minster, T.H. Jordan, Present-day plate motions, *J. Geophys. Res.* 83 (1978) 5331–5354.
- [2] C. DeMets, R.G. Gordon, D.F. Argus, S. Stein, Current plate motion, *Geophys. J. Int.* 101 (1990) 425–478.
- [3] C. DeMets, R.G. Gordon, D.F. Argus, S. Stein, Effects of recent revisions to the geomagnetic reversal time scale on estimates of current plates motions, *Geophys. Res. Lett.* 21 (1994) 2191–2194.
- [4] R. Searle, Tectonic pattern of the Azores spreading center and triple junction, *Earth Planet. Sci. Lett.* 51 (1980) 415–434.
- [5] P. Lonsdale, Structural pattern of the Galapagos microplate and evolution of the Galapagos triple junction, *J. Geophys. Res.* 93 (1988) 13551–13574.
- [6] R.L. Larson, R.C. Searle, M.C. Kleinrock, H. Schouten, R.T. Bird, D.F. Naar, R.I. Rusby, E.E. Hooft, H. Lashiotakis, Roller-bearing tectonic evolution of the Juan Fernandez microplate, *Nature* 356 (1992) 571–576.
- [7] M. Ligi, E. Bonatti, G. Bortoluzzi, G. Carrara, P. Fabbretti, D. Penitenti, D. Gilod, A.A. Peyve, S. Skolotnev, N. Turko, Death and transfiguration of a triple junction in the South Atlantic, *Science* 276 (1997) 243–245.
- [8] N.C. Mitchell, R.A. Livermore, The present configuration of the Bouvet triple junction, *Geology* 26 (1998) 267–270.
- [9] N.C. Mitchell, Distributed extension at the Indian Ocean triple junction, *J. Geophys. Res.* 96 (1991) 8019–8043.
- [10] D. Sauter, V. Mendel, C. Rommevaux-Jestin, P. Patriat, M. Munsch, Propagation of the southwest Indian Ridge at the Rodrigues triple junction, *Mar. Geophys. Res.* 19 (1997) 553–567.
- [11] R.G. Gordon, C. DeMets, Present-day motion along the Owen fracture zone and Dalrymple trough in the Arabian Sea, *J. Geophys. Res.* 94 (1989) 5560–5570.
- [12] C.G. Chase, Plate kinematics: the Americas, East Africa and the rest of the world, *Earth Planet. Sci. Lett.* 37 (1978) 355–368.
- [13] J.R. Cochran, The Gulf of Aden: structure and evolution of a young ocean basin and continental margin, *J. Geophys. Res.* 86 (1981) 263–287.
- [14] F. Jestin, P. Huchon, J.M. Gaulier, The Somalia plate and the East African rift system: Present-day kinematics, *Geophys. J. Int.* 116 (1994) 637–654.
- [15] I. Manighetti, P. Tapponnier, V. Courtillot, S. Gruszow, P.Y. Gillot, Propagation of rifting along the Arabia–Somalia plate boundary: The Gulfs of Aden and Tadjoura, *J. Geophys. Res.* 102 (1997) 2681–2710.
- [16] R.C. Quittmeyer, A.L. Kafka, Constraints on plate motions in southern Pakistan and the northern Arabian Sea from the focal mechanisms of small earthquakes, *J. Geophys. Res.* 89 (1984) 2444–2458.
- [17] A.M. Dziewonski, G. Ekström, M.P. Salganik, Centroid-moment tensor solutions for April–June 1998, *Phys. Earth Planet. Int.* 104 (1999) 11–20.
- [18] D. Tamsett, R. Searle, Structure of the Alula–Fartak fracture zone, Gulf of Aden, *J. Geophys. Res.* 95 (1990) 1239–1254.
- [19] M. Withjack, W. Jamison, Deformation produced by oblique rifting, *Tectonophysics* 126 (1986) 99–124.
- [20] O. Dauteuil, J.P. Brun, Oblique rifting in a slow-spreading ridge, *Nature* 361 (1993) 145–148.
- [21] G.W. Tuckwell, J.M. Bull, D.J. Sanderson, Models of fracture orientation at oblique spreading centres, *J. Geol. Soc. Lond.* 153 (1996) 185–189.
- [22] J.W. Morgan, Rises, trenches, great faults, and crustal blocks, *J. Geophys. Res.* 73 (1968) 1959–1982.
- [23] V.Y. Glebovsky, S.P. Maschenkov, A.M. Gorodnitsky, I.I. Belyaev, A.M. Filin, S.V. Mercuriev, N.A. Sochevanova, S.V. Lukyanov, G.M. Valyashko, E.A. Popov, K.V. Popov, Mid-oceanic ridges and deep oceanic basins: AMF structure, in: A.M. Gorodnitsky (Ed.), *Anomalous Magnetic Field of the World Ocean*, CRC Press, Boca Raton, FL, 1995, pp. 67–144.
- [24] S. Mercuriev, P. Patriat, N. Sochevanova, Evolution de la dorsale de Carlsberg évidence pour une phase d'expansion très lente entre 40 et 25 Ma (A18 à A7), *Oceanol. Acta* 19 (1996) 1–13.
- [25] L. Audin, Pénétration de la dorsale d'Aden dans la dépression Afar entre 20 et 4 Ma, PhD Thesis, Université Paris 7, 1999, 300 pp.
- [26] H. Hébert, C. Deplu, P. Huchon, K. Khanbari, L. Audin, Lithospheric structure of a nascent spreading ridge

- inferred from gravity data: the western Gulf of Aden, *J. Geophys. Res.*, in press.
- [27] P. Patriat, Reconstruction de l'évolution du système de dorsales de l'Océan indien par les méthodes de la cinématique des plaques, *Terres Australes et Antarctiques Françaises*, Paris, 1987, 308 pp.
- [28] D.T. Sandwell, W.H.F. Smith, Marine gravity anomaly from Geosat and ERS-1 satellite altimetry, *J. Geophys. Res.* 102 (1997) 10039–10054.
- [29] G. Sahota, Geophysical investigation of the Gulf of Aden continental margins: geodynamic implications for the development of the Afro-Arabian rift systems, PhD Thesis, University Of Wales, Swansea, 1990, 242 pp.
- [30] F. Watchorn, G.J. Nichols, D.W.J. Bosence, Rift-related sedimentation and stratigraphy, southern Yemen (Gulf of Aden), in: B.H. Purser, D.W.J. Bosence (Eds.), *Sedimentation and Tectonics of Rift Basins: Red Sea-Gulf of Aden*, Chapman and Hall, London, 1998, pp. 165–191.
- [31] D.P. McKenzie, W.J. Morgan, Evolution of triple junctions, *Nature* 224 (1969) 125–133.
- [32] N.L. Grimson, W.-P. Chen, The Azores-Gibraltar plate boundary: focal mechanisms, depths of earthquakes, and their tectonic implications, *J. Geophys. Res.* 91 (1986) 2029–2047.
- [33] D.F. Argus, R.G. Gordon, C. DeMets, S. Stein, Closure of the Africa-Eurasia-North America plate motion circuit and tectonics of the Gloria fault, *J. Geophys. Res.* 94 (1989) 5585–5602.
- [34] J. Freire Luis, J.M. Miranda, A. Galdeano, P. Patriat, J.C. Rossignol, L.A. Mendes Victor, The Azores triple junction evolution since 10 Ma from an aeromagnetic survey of the Mid-Atlantic Ridge, *Earth Planet. Sci. Lett.* 125 (1994) 439–459.
- [35] S.P. Srivastava, H. Schouten, W.R. Roest, K.D. Klitgord, L.C. Kovacs, J. Verhoef, R. Macnab, Iberian plate kinematics: a jumping plate boundary between Eurasia and Africa, *Nature* 344 (1990) 756–759.
- [36] P. Wessel, W.M.F. Smith, Free software helps map and display data, *EOS Trans. AGU* 72 (1991) 441–446.